

This is in response to the Final Office Action mailed June 20, 2007. Claims 1-28 are presently pending. The Applicant thanks the Examiner for indicating that claim 27 would be allowable if rewritten in independent form. The Applicant requests entry of this response in view of the new rejections of the present claims.

§103 Rejections

Claims 1 and 13 recite a laser comprising a passive negative feedback (PNF) element and a saturable absorber (SA) element that has an absorption recovery time which is longer than an output pulse duration. Claim 1 also recites that a location of the SA element is variable so that the SA element can be positioned between different pairs of other components of the laser and the output pulse duration can be varied by varying location of the SA element. Claim 13 recites varying a position of the SA element so that the SA element is sequentially positioned between different pairs of other components of the laser, whereby the output pulse duration is varied.

{S:\04379\000m882us0\80120700.DOC }

SA). Office Action, p.3. The Office Action turns to Il'ichev which describes a slow SA and asserts that one of skill in the art would modify Del Corno to include the SA of Il'ichev and, thereby, render the inventions of claims 1 and 13 obvious.

First, the Applicant respectfully submits that one of skill in the art would not combine Del Corno and Il'ichev as suggested in the Office Action. Del Corno discloses an active-passive mode locked Nd:YAG laser. The Del Corno laser utilizes a dye cell that acts as a saturable absorber. The dye cell is a fast SA with an absorption recovery time (6-9 ps - see p. 960, Col. 2, lines 5-7 of accompanying article by von der Linde et al., IEEE Journal of Quantum Electronics, 9, 960-1 (1970)), that is shorter than the output pulse duration (10-30 ps). The Del Corno laser uses the passive mode-locking capabilities of the fast SA. Passive mode locking using a SA requires that the absorption recovery time of the SA is shorter than the output pulse duration. (See, p. 531, third full paragraph of W. Koechner, "Solid-State Laser Engineering", Chapter 9.2 Passive Mode Locking, Springer Verlag (1999) and p. 960, first paragraph of von der Linde, et al., IEEE Journal of Quantum Electronics, 9, 960-1 (1970), both of which accompany this Response.)

In contrast, a slow SA, such as that described in Il'ichev, does not passively mode-lock. The Cr^{4+} :YAG crystal of Il'ichev has an absorption lifetime on the order of 3-8 μs (see, e.g., p. 3, lines 18-19 of the present patent application.) This is substantially longer than the picosecond pulses described in the present patent application or in Del Corno and much longer than the approximately 10-100 ns roundtrip time for the resonator. The slow SA can be used for Q-switching, as described in Il'ichev, but it will not provide passive mode-locking.

Accordingly, one of skill in the art would not consider it obvious to utilize the slow SA absorber of Il'ichev to modify the laser of Del Corno because he Del Corno laser utilizes the passive mode-locking capabilities of the fast SA. The slow SA of Il'ichev can not provide passive mode-locking. Bai uses the same Cr^{4+} :YAG SA as Il'ichev and so does not address these deficiencies of Del Corno and Il'ichev.

Second, in contrast to the assertion in the Office Action, Bai does not teach or suggest positioning the SA element between different pairs of components of the laser as recited in claims 1 and 13. Bai only discloses small variations in position of the SA away from the output coupler (OC of Fig. 1 of Bai.) Bai, p. 2470, first partial paragraph. Thus, the SA element is always between the output coupler (OC of Fig. 1) and the concave curved mirror (CM of Fig. 1). Moreover, the variation in distance is only at most 7 mm of the 3.5 cm (see, Bai, Fig. 1) distance between OC and CM. Bai, p. 2470, Col. 2, lines 4-5 and Fig. 1.

Finally, Bai teaches against positioning the SA between any components other than the OC and CM. In particular, Bai states: “When the saturable absorber was placed in the long arm of the laser, Q-switched pulses were never observed....” Bai, p. 2469, Col. 2, lines 21-30. The only components in the short arm of the laser, where the SA is positioned according to Bai, are the OC, SA, and CM.

Accordingly, Bai fails to teach or suggest positioning the SA element between different pairs of components of the laser as recited in claims 1 and 13. The other references do not address these deficiencies of Bai.

Therefore, Del Corno, Il’ichev, and Bai, alone or in combination, fail to teach or suggest every element of the claims. For at least these reasons, claims 1 and 13, as well as claims 2-12 and 14-27 which depend therefrom, are patentable over the cited references. The Applicants respectfully request withdrawal of the rejections of these claims.

With respect to claim 28, the Office Action acknowledges that Del Corno, Il’ichev, and Bai do not teach that the SA is located between the PNF element and the AOML as recited in claim 28. Office Action, p. 5. The Office Action asserts that placement of the SA between the PNF and the AOML is a matter of design and would be obvious to one of ordinary skill in the art.

The Applicant respectfully submits that placement of components within a laser cavity are not necessarily simply a matter of design, but instead may substantially impact the operation of

5

Only the last term (the 1 in the last bracket) is the contribution of the ∇n^2 term of the wave equation (2).

GROUP VELOCITY

The term with Δ/k in (15) is usually very small for small values of p so that the change of the propagation constant, that is caused by the ∇n^2 term of the wave equation, is not very significant. However, its contribution to the group velocity is of more importance. We obtain the inverse group velocity $1/v$ with the help of (15)

$$\frac{1}{v} = \frac{1}{c} \frac{d\beta}{dk} = \frac{n_0}{c} \left\{ 1 + \frac{\Delta}{n_0 k a} [(p + \frac{1}{2})^2 + 1] \right\} \quad (16)$$

so that the group velocity assumes the approximate form

$$v = \frac{c}{n_0} \left\{ 1 - \frac{\Delta}{(n_0 k a)^2} [(p + \frac{1}{2})^2 + 1] \right\}. \quad (17)$$

For the lowest order mode with $p = 1$ the ∇n^2 term causes a change in $v = c/n_0$ of 44 percent. For the second-order mode with $p = 2$ this change is only 16 percent and decreases rapidly with increasing mode number.

CONCLUSIONS

We have studied the influence of the ∇n^2 term on the propagation constants of the modes of the square-law medium. We conclude from this investigation that this term has a slight influence on the group velocity of the lowest order modes. However, for these modes the group velocity is very nearly equal to c/n_0 so that the slight change of the additional term is not very important. For higher order modes the influence of the ∇n^2 term becomes even less significant. Thus we conclude that the solutions of the reduced wave equation (3) provide an approximation to the solutions of the exact wave equations (1) or (2) that is sufficiently accurate for most practical applications.

REFERENCES

- [1] D. Marcuse, *Light Transmission Optics*. New York: Van Nostrand-Reinhold, 1972.
- [2] M. Matsuhara, "Analysis of electromagnetic-wave modes in lens-like media," *J. Opt. Soc. Amer.*, vol. 63, pp. 135-145, Feb. 1973.
- [3] L. I. Schiff, *Quantum Mechanics*. New York: McGraw-Hill, 1955.

Recovery Time of Saturable Absorbers for 1.06 μ

D. VON DER LINDE AND K. F. RODGERS

Abstract—The recovery time of a new saturable absorber suitable for mode locking of neodymium lasers has been measured and compared with the recovery of two commonly used saturable dyes (Eastman 9740 and 9860).

The prospect of obtaining picosecond and subpicosecond light pulses of high power from passively mode-locked lasers has created interest in saturable absorbers having recovery times of the order of 10^{-12} s or shorter. For example, to achieve complete mode locking

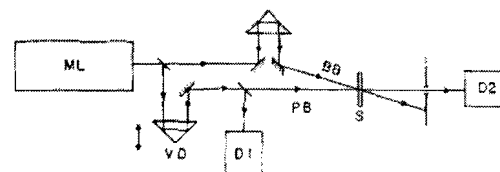


Fig. 1. Schematic of the experimental system: Mode-locked Nd: glass laser ML; variable optical delay for the probe beam VD; sample S; photodetectors D1 and D2; bleaching beam BB; probe beam PB.

of the total gain-bandwidth of Nd: glass lasers ($\Delta\nu_g \approx 3 \times 10^{12} \text{ s}^{-1}$) a saturable absorber with a recovery time $\tau \approx 1/\Delta\nu_g \approx 0.3 \times 10^{-12} \text{ s}$ is needed. The relaxation of two commonly used saturable dyes for $\lambda = 1.06 \mu$ (Kodak 9740 and 9860) has been studied previously by several workers under different experimental conditions. The relaxation times of the relevant excited states were found to be approximately 10^{-11} s (8–25 ps for 9740 [1], [3], and 6–9 ps for 9860 [2], [3]). During the search for faster relaxing systems, we have investigated the recovery of a new saturable dye (dye 1) of similar structure which was believed by the manufacturer to have a very short recovery time.¹ We also have remeasured the recovery of 9740 (dye 2) and 9860 (dye 3) for the same experimental conditions to allow a comparison of the three saturable dyes.

Our experimental method is similar to techniques used previously for the measurement of the recovery of saturable absorbers [1], [2], and for the study of vibrational lifetimes [4]. The experimental system is shown in Fig. 1. An intense pulse train (pulse separation 10 ns) from a mode-locked Nd: glass laser is used to saturate the absorption of the dye solution under study. A small fraction ($\approx 10^{-2}$) of the same pulse train serves as a probe for measuring the transmission of the sample at various delay times after excitation by the strong beam. Care was taken to maintain complete spatial overlap of the cross section of the probe beam with the pumped volume of the sample when the probe delay was changed. In order to measure the transmission at constant bleaching conditions, we measured only one pulse out of the total incident probe train, and the corresponding pulse in the transmitted train for evaluation of the transmission. This pair of pulses was chosen from the very front of the pulse train, and the energy of the selected bleaching pulse was kept constant to within 10 percent. The pulse energy was measured with a detection system of 500-ps time resolution.

The selection of a single pulse ensured that we were working with well-defined light pulses of about 5–6-ps duration with approximately Gaussian shape [5]. The peak power density of the bleaching pulses was about 300 MW/cm^2 . The measurements were performed with solutions of the dyes in dichloroethane, adjusted to an initial transmission of $T_0 = 2$ percent. Irradiating the samples with bleaching pulses of 300 MW/cm^2 increased the transmission to approximately 40 percent. The maximum transmission was observed at a delay time of about 10 ps. At larger delay times the transmission decreased and approached the initial value T_0 with a characteristic time constant. The measured transmission curves for the three dyes are shown in Fig. 2. The logarithm of the normalized energy transmission, $\ln(T/T_0)$, is plotted versus delay time t_d . The experimental points represent an average value of typically 15 measurements. The error bars indicate the respective standard deviations. The measured energy transmission is related to the convolution of the probe pulse with the instantaneous transmittance induced by the strong pump pulse. For excitation and probing by Gaussian-shaped pulses, the convolution at long delays directly traces the decay of the material excitation, even if the pulse duration t_p is of the same order as the decay time τ [4] (in the present experiment: $t_p/\tau \lesssim 0.9$). The measurements indicate an exponential

Manuscript received May 11, 1973.
The authors are with Bell Laboratories, Murray Hill, N.J. 07974.

¹ We are grateful to K. M. Drexhage of Eastman Kodak for making their new dye (1) available to us.

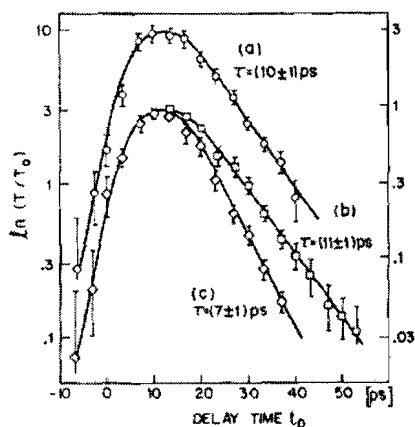


Fig. 2. Logarithm of the measured transmission as a function of the delay t_0 of the probe pulse. (a) Dye 1 (right scale). (b) Dye 2 (9740, left scale). (c) Dye 3 (9860, left scale).

decay of the concentration of excited molecules for $t_0 > 20$ ps, and the recovery times of the absorbers are obtained from the slope of the respective transmission curve. Accurate values of τ were obtained in the present experiment because a decay by more than a

factor of 10 of the number of excited molecules has been measured. It turned out that dye 1 recovers only slightly faster than 9740: We found $\tau = (10 \pm 1)$ ps for dye 1, and $\tau = (11 \pm 1)$ ps for 9740. For 9860 we measured $\tau = (7 \pm 1)$ ps.

Measurement of the dependence of absorption saturation on the incident power showed that the three dyes all have the same saturation characteristic (within experimental accuracy $\Delta T = \pm 5$ percent). This result confirms that the recovery times are very similar (the absorption cross sections do not differ significantly).

No information on structural details of the studied dyes was available. Therefore, an interpretation of the measured differences of the recovery times is not possible at the present time.

REFERENCES

- [1] J. W. Shelton and J. A. Armstrong, "Measurement of the relaxation time of the Eastman 9740 bleachable dye," *IEEE J. Quantum Electron. (Corresp.)*, vol. QE-3, pp. 696-697, Dec. 1967.
- [2] R. I. Scarlet, J. F. Figueroa, and H. Mahr, "Direct measurement of picosecond lifetimes," *Appl. Phys. Lett.*, vol. 13, p. 71, 1968.
- [3] M. M. Malley and P. M. Rentzepis, "Picosecond molecular relaxation displayed with crossed laser beams," *Chem. Phys. Lett.*, vol. 3, p. 534, 1969; also M. R. Topp, P. M. Rentzepis, and R. P. Jones, "Time-resolved absorption spectroscopy in the 10^{-12} sec range," *J. Appl. Phys.*, vol. 42, p. 3415, 1971.
- [4] D. von der Linde, A. Laubereau, and W. Kaiser, "Molecular vibrations in liquids: Direct measurement of the molecular dephasing time; Determination of the shape of picosecond light pulses," *Phys. Rev. Lett.*, vol. 26, p. 954, 1971.
- [5] D. von der Linde, "Experimental study of single picosecond light pulses," *IEEE J. Quantum Electron.*, vol. QE-8, pp. 328-338, Mar. 1972.

Springer Series in Optical Sciences

Editorial Board: A. L. Schawlow† A. E. Siegman T. Tamir

- 42 **Principles of Phase Conjugation**
By B. Ya. Zel'dovich, N. F. Pilipetsky,
and V. V. Shkunov
- 43 **X-Ray Microscopy**
Editors: G. Schmahl and D. Rudolph
- 44 **Introduction to Laser Physics**
By K. Shimoda 2nd Edition
- 45 **Scanning Electron Microscopy**
Physics of Image Formation and Microanalysis
By L. Reimer 2nd Edition
- 46 **Holography and Deformation Analysis**
By W. Schumann, J.-P. Zuercher, and D. Cuche
- 47 **Tunable Solid State Lasers**
Editors: P. Hammering, A. B. Budgor,
and A. Pinto
- 48 **Integrated Optics**
Editors: H. P. Nothling and R. Ulrich
- 49 **Laser Spectroscopy VII**
Editors: T. W. Hänsch and Y. R. Shen
- 50 **Laser-Induced Dynamic Gratings**
By H. J. Eichler, P. Günter, and D. W. Pohl
- 51 **Tunable Solid State Lasers for Remote Sensing** Editors: R. L. Byer, E. K. Gustafson,
and R. Trebino
- 52 **Tunable Solid-State Lasers II**
Editors: A. B. Budgor, L. Esterowitz,
and L. G. DeShazer
- 53 **The CO₂ Laser** By W. J. Witteman
- 54 **Lasers, Spectroscopy and New Ideas**
A Tribute to Arthur L. Schawlow
Editors: W. M. Yen and M. D. Levenson
- 55 **Laser Spectroscopy VIII**
Editors: W. Persson and S. Svanberg
- 56 **X-Ray Microscopy II**
Editors: D. Sayre, M. Howells, J. Kirz,
and H. Karbach
- 57 **Single-Mode Fibers Fundamentals**
By E. G. Neumann
- 58 **Photoacoustic and Photothermal Phenomena**
Editors: P. Hess and J. Peřl
- 59 **Photorefractive Crystals in Coherent Optical Systems**
By M. P. Petrov, S. I. Stepanov,
and A. V. Khomenko
- 60 **Holographic Interferometry in Experimental Mechanics**
By Yu. I. Ostrovsky, V. P. Stetshepinov,
and V. V. Yakovlev
- 61 **Millimetre and Submillimetre Wavelength Lasers** A Handbook of cw Measurements
By N. G. Douglas
- 62 **Photoacoustic and Photothermal Phenomena II**
Editors: J. C. Murphy, J. W. MacLachlan Spicer,
L. C. Aamodt, and B. S. H. Royce
- 63 **Electron Energy Loss Spectrometers**
The Technology of High Performance
By H. Ibach
- 64 **Handbook of Nonlinear Optical Crystals**
By V. G. Dmitriev, G. G. Gurzadyan,
and D. N. Nikogosyan 3rd Edition
- 65 **High-Power Dye Lasers**
Editor: F. J. Duarte
- 66 **Silver Halide Recording Materials for Holography and Their Processing**
By H. I. Bjelkhagen 2nd Edition
- 67 **X-Ray Microscopy III**
Editors: A. G. Michette, G. R. Morrison,
and C. J. Buckley
- 68 **Holographic Interferometry Principles and Methods**
Editor: P. K. Rastogi
- 69 **Photoacoustic and Photothermal Phenomena III**
Editor: D. Břčanec
- 70 **Electron Holography**
By A. Tonomura 2nd Edition
- 71 **Handbook of Energy-Filtering Transmission Electron Microscopy**
Editor: L. Reimer
- 72 **Handbook of Nonlinear Optical Effects and Materials**
Editor: P. Günter
- 73 **Evanescent Waves**
By F. de Fornel
- 74 **International Trends in Optics and Photonics ICO IV**
Editor: T. Asakura

Volumes 1-41 are listed at the end of the book

Walter Koechner

Solid-State Laser Engineering

Fifth Revised and Updated Edition

With 472 Figures and 55 Tables



Springer

Dr. WALTER KOECHNER

Fibertek, Inc., 510 Herndon Parkway
Herndon, VA 20170, USA
Wkoechner@aol.com

Editorial Board

ARTHUR L. SCHAWLOW†, Ph.D.

Department of Physics, Stanford University
Stanford, CA 94305-4060, USA

THEODOR TAMIR, Ph.D.

Department of Electrical Engineering
Polytechnic University, 333 Jay Street
Brooklyn, NY 11202, USA

Professor ANTHONY E. SIEGMAN, Ph.D.

Electrical Engineering

E. L. Ginzton Laboratory, Stanford University
Stanford, CA 94305-4085, USA

Library of Congress Cataloging-in-Publication Data

Koechner, Walter, 1937-. Solid-state laser engineering / Walter Koechner. -

5th rev. and updated ed.

p. cm. - (Springer series in optical sciences; v. 1)

Includes bibliographical references and index. ISBN 3-540-65064-4 (alk. paper)

1. Solid-state lasers. I. Title. II. Series. TA1705.K63 1999 621.36'61-dc21 99-15546 CIP

ISBN 3-540-65064-4 Springer-Verlag Berlin Heidelberg New York
ISBN 3-540-60237-2 4th edition Springer-Verlag Berlin Heidelberg New York

This work is subject to copyright. All rights are reserved, whether the whole or part of the material is concerned, specifically the rights of translation, reprinting, reuse of illustrations, recitation, broadcasting, reproduction on microfilm or in any other way, and storage in data banks. Duplication of this publication or parts thereof is permitted only under the provisions of the German Copyright Law of September 9, 1965, in its current version, and permission for use must always be obtained from Springer-Verlag. Violations are liable for prosecution under the German Copyright Law.

© Springer-Verlag Berlin Heidelberg 1976, 1988, 1992, 1996, 1999

Printed in Germany

The use of general descriptive names, registered names, trademarks, etc. in this publication does not imply, even in the absence of a specific statement, that such names are exempt from the relevant protective laws and regulations and therefore free for general use.

Typeset in TeX by K. Steingraeber, Heidelberg, using a Springer TeX macro-package
Cover concept by cStudio Calamar Steinen using a background picture from The Optics Project,
Courtesy of John T. Foley, Professor, Department of Physics and Astronomy, Mississippi State
University, USA

Cover production: design & production GmbH, Heidelberg

Printed on acid-free paper

SPIN 10695027

56/3144-543210

Preface to the Fifth Edition

This book, written from an industrial vantage point, provides a detailed discussion of solid-state lasers, their characteristics, design and construction, and practical problems. The title *Solid-State Laser Engineering* has been chosen because the emphasis is placed on engineering and practical considerations of solid-state lasers. I have tried to enhance the description of the engineering aspects of laser construction and operation by including numerical and technical data, tables, and curves.

The book is mainly intended for the practicing scientist or engineer who is interested in the design or use of solid-state lasers, but the response from readers has shown that the comprehensive treatment of the subject makes the work useful also to students of laser physics who want to supplement their theoretical knowledge with the engineering aspects of lasers. Although not written in the form of a college textbook, the book might be used in an advanced college course on laser technology.

The aim was to present the subject as clearly as possible. Phenomenological descriptions using models were preferred to an abstract mathematical presentation, even though many simplifications had then to be accepted. Results are given in most cases without proof since I have tried to stress the application of the results rather than the derivation of the formulas. An extensive list of references is cited for each chapter to permit the interested reader to learn more about a particular subject.

Again, gratified by the wide acceptance of the previous edition of *Solid-State Laser Engineering*, I have updated and revised the fifth edition to include developments and concepts which have emerged during the last several years. Since the publication of the fourth edition, continued dramatic changes have taken place in the development of solid-state lasers. Today, systems range from tiny, diode-pumped micro-chip lasers to stadium-sized Nd:glass lasers under construction at the National Ignition Facility. The combination of diode-pump sources with innovative pump and resonator designs has dramatically improved beam quality obtainable from solid-state lasers. Spectral coverage, and output power at different wavelengths, have been considerably increased as a result of the emergence of improved nonlinear crystals. Also, table-top femtosecond laser sources have become a reality. At the high end of the power range, flashlamp-pumped Nd:YAG lasers up to the 5 kW level are employed for welding applications, and a number of diode-pumped lasers with outputs in the kW range have been demonstrated at various laboratories. For military and spaceborne systems, where compact pack-

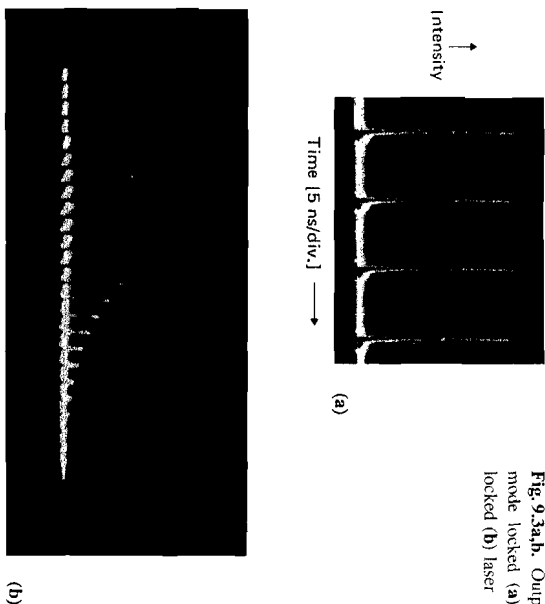


Fig. 9.3a,b. Output pulses from a cw mode-locked (a) and a pulsed mode-locked (b) laser

following sections. Excellent tutorial discussions of the work on mode-locked lasers with extensive references can be found in [9.2–6].

9.2 Passive Mode Locking

The nonlinear absorption of saturable absorbers was first successfully employed for simultaneously Q-switching and mode-locking solid-state lasers in 1965 [9.7, 8]. The saturable absorbers consisted of organic dyes that absorb at the laser wavelength. At sufficient intense laser radiation, the ground state of the dye becomes depleted, which decreases the losses in the resonator for increasing pulse intensity.

In pulsed mode-locked solid-state lasers, pulse shortening down to the limit set by the gain-bandwidth is prevented because of the early saturation of the absorber which is a result of the simultaneously occurring Q-switching process. Shorter pulses and a much more reproducible performance is obtained if the transient behavior due to Q-switching is eliminated. In steady-state or cw mode locking, components or effects are utilized which exhibit a saturable absorber-like behavior, i.e. a loss that decreases as the laser intensity increases. In this section, we will review pulsed and cw passive mode locking.

9.2.1 Pulsed Passive Mode Locking

As mentioned in Chap. 8, a saturable absorber has a decreasing loss for increasing pulse intensities. The distinction between an organic dye suitable for simultaneous mode-locking and Q-switching, as opposed to only Q-switching the laser, is the recovery time of the absorber. If the relaxation time of the excited-state population of the dye is on the order of the cavity round trip, i.e. a few nanoseconds, passive Q-switching will occur, as described in Chap. 8.

With a dye having a recovery time comparable to the duration of mode-locked pulses, i.e. a few picoseconds, simultaneous mode-locking and Q-switching can be achieved. Fast recovery times usually arise from non-radiative decay in the dyes, whereas the slower relaxation times are due to spontaneous emission.

We will now discuss the pulse formation in a passively mode-locked laser. A computer simulation of the evolution of a mode-locked pulse train from noise is shown in Fig. 9.4 [9.9]. This figure shows the transformation of irregular pulses into a single mode-locked pulse. In Figs. 9.4a–c the noise-like fluctuations are linearly amplified, however, a smoothing and broadening of the pulse structure can be seen. In Figs. 9.4d–f the peak-to-peak excursions of the fluctuations have increased and, in particular, the amplitude of the strongest pulse has been selectively emphasized. In Fig. 9.4f the background pulses have been completely suppressed.

The simultaneous Q-switched and mode-locked pulse evolution from noise can be divided into several stages.

Linear Amplification Stage. At the beginning of the flashlamp pulse, the laser gain is not high enough to overcome the loss of the saturable absorber. Population inversion of the laser transition and the transmission of the bleachable dye are not affected by the radiation. As a result, both the amplification and absorption processes can be considered to be linear. The intensity pattern is that of spontaneous emission with a spectral content about equal to the fluorescence bandwidth. Interference of the laser modes with random phase relations leads to fluctuations of the light intensity. The total number of fluctuations is large, being of the order of the number of cavity modes, but there is a small number of intensity peaks exceeding the average intensity significantly. The chaotic sequence of fluctuations shown in Fig. 9.4a represents the laser radiation in the early stage of pulse generation.

As the pump process continues, the gain increases above threshold and the noise-like signal is amplified. During the linear amplification a natural mode selection takes place because the frequency-dependent gain favors cavity modes in the center of the fluorescence line. As a result of the spectral narrowing caused by the amplification process, a smoothing and broadening of the amplitude fluctuations occurs, as shown in Figs. 9.4b and c.

The following numbers are typical for the linear amplification process in Nd:glass. A large number of longitudinal modes is initially excited. For a typical cavity length of ~ 1 m, one calculates $\sim 4 \times 10^4$ cavity modes in Nd:glass with

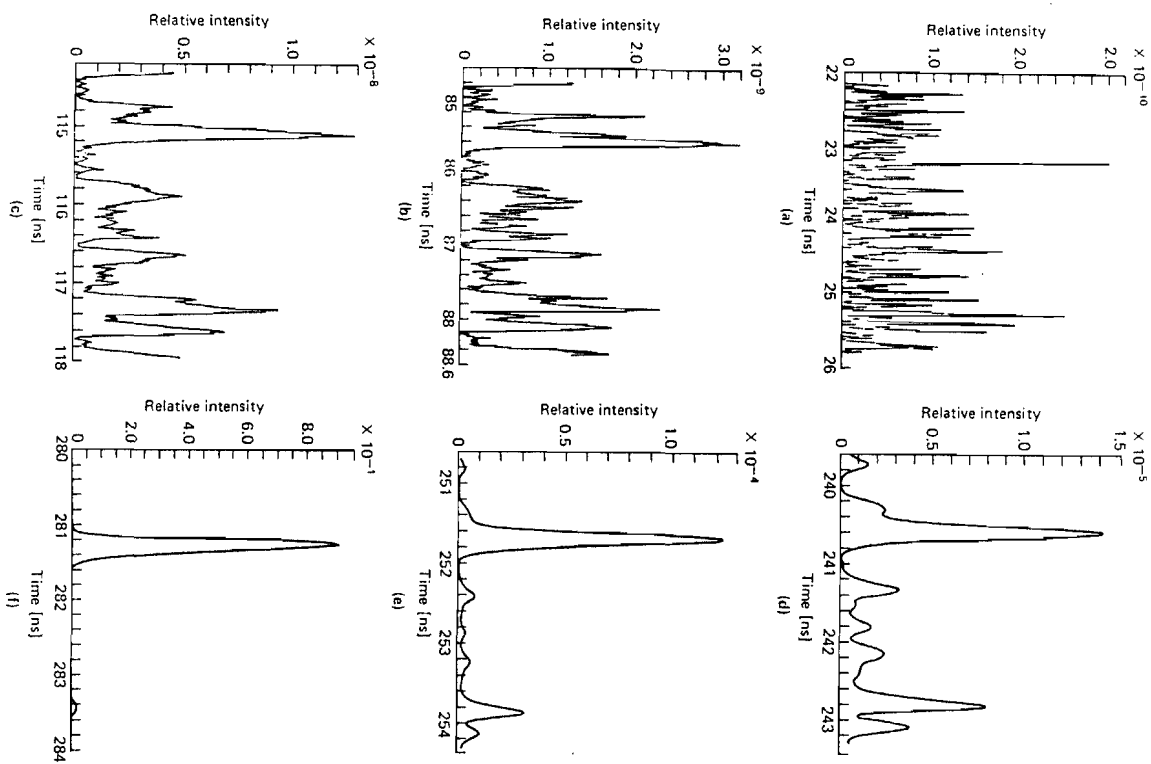


Fig. 9.4a-f. Computer simulation of the evaluation of a mode-locked pulse from noise. (a-c) regime of linear amplification and linear dye absorption, (d-e) nonlinear absorption in the dye cell, (f) regime of nonlinear amplification, dye completely bleached [9.9]

$\delta\nu_F \approx 7500$ GHz. Assuming a typical pulse build-up time of $10 \mu\text{s}$, the linear stage comprises ≈ 1500 round trips. The light intensity rises by many orders of magnitude to approximately 10^7 W/cm^2 .

Nonlinear Absorption. In this second phase of pulse evolution, the gain is still linear but the absorption of the dye cell becomes nonlinear because the intensity peaks in the laser cavity approach values of the saturation intensity I_s of the dye (Fig. 8.26). In the nonlinear regime of the mode-locked laser we note two significant processes acting together:

First, there is a selection of one peak fluctuation or at least a small number. The most intense fluctuations at the end of the linear amplification phase preferentially bleach the dye and grow quickly in intensity. The large number of smaller fluctuations, on the contrary, encounter larger absorption in the dye cell and are effectively suppressed.

The second effect is a narrowing of the existing pulses in time, which broadens the frequency spectrum. The shapes of the pulses are affected by the nonlinearity of the dye because the wings of the pulse are more strongly absorbed than the peak. The second phase ends when the absorbing transition in the dye cell is completely saturated. Under favorable conditions the final transmission is close to one; i.e., the dye is transparent. The nonlinear action of the absorber at the intermediate power regime was illustrated in Figs. 9.4d and e.

Nonlinear Amplification. The final phase of the pulse evolution occurs when the intensity is sufficiently high for complete saturation of the absorber transition to take place and for the amplification to be nonlinear. This is the regime of high peak power. During the nonlinear stage the pulse intensity quickly rises within ≈ 50 cavity round trips to a value of several gigawatts per square centimeter. As was shown in Fig. 9.4f, at this point the background pulses have been almost completely suppressed. Successive passages of the high-intensity radiation pulse through the resonator result in a pulse train appearing at the laser output. Finally, the population inversion is depleted and the pulse decays.

The design elements of interest in pulsed passive mode-locked lasers are the resonator configuration, dye cell, and the gain media.

Resonator. One major requirement in the resonator design of a mode-locked system is the complete elimination of reflections which can occur from components located between the two cavity mirrors. This is accomplished by employing laser rods with Brewster's angle at the ends, placing the dye cell at Brewster's angle in the resonator, and by using cavity mirrors which are wedged. Reflection from an optical surface which is parallel to the cavity mirrors will create a secondary resonator. The mode-locked pulse will be split into several pulses which will circulate inside the resonators with different round-trip times. The result is a very erratic output usually consisting of several superpositioned pulse trains or containing subsidiary pulses in the train. With all optical surfaces inside the

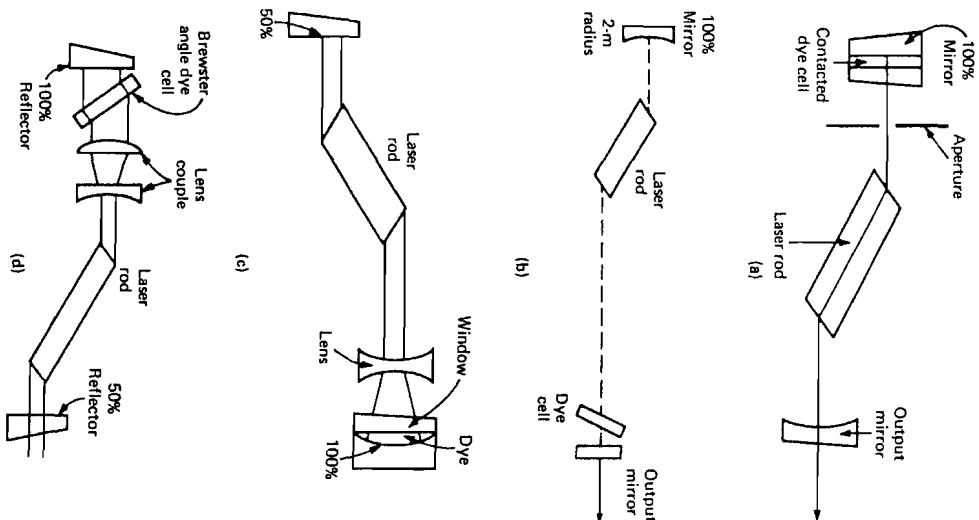


Fig. 9.5a-d. Experimental arrangements for passively mode-locked lasers. Oscillator cavity with optically contacted dye cell (a) and with dye cell tilted at Brewster angle (b) arrangements, including telescopes in the resonator, are shown in (c) and (d).

resonator, either at Brewster angle or antireflection-coated and tilted away from the resonator axis, coupled resonator structures can be avoided and the occurrence of satellite pulses is minimized. Similar attention must be paid to avoid back-reflection into the cavity from external components.

Figure 9.5 shows various configurations of mode-locked oscillators. In order to reduce the number of reflective surfaces in the laser cavity and, therefore,

minimize the possibility of secondary reflections, the dye cell and rear mirror are often combined. As shown in Fig. 9.5a, the 100% mirror takes the place of the rear dye-cell window. A saturable absorber, where the dye is in contact with the cavity mirror, not only provides the most reliable mode-locking operation but also yields the shortest pulses. Typically, dye cells vary in length from 1 cm to 0.1 cm. However, it has been found that the width of the individual pulses in a mode-locked train have a direct relationship to the optical path length of the dye cell. The most reliable mode locking and the shortest pulses are obtained when the saturable absorber is placed in contact with one of the dielectric mirrors and the dye thickness l satisfies the condition $l \leq c\tau/2n$, where τ and n are the relaxation time and refractive index of the dye, respectively, and c is the speed of light. For Eastman dyes A9740 and A9860, $l \approx 1$ mm. The relationship between dye thickness and pulse duration has been investigated in [9, 10] and the shortest pulses have been measured for $l \approx 30 \mu\text{m}$.

The resonator length is usually chosen between 1 and 1.5 m; in this case the pulse separation is of the order of 10 ns, which makes the selection of a single pulse with an external gate relatively simple. The reflectivity of the front mirror is typically between 50 and 60%. The output reproducibility from a mode-locked laser is drastically improved by using at least one curved mirror instead of two plane mirrors. Very often a mode-selecting aperture is inserted into the resonator of a mode-locked oscillator because in multitransverse-mode systems the power density is so large in localized areas that component damage frequently occurs. Sometimes a Galilean telescope or a single lens is included in the laser cavity to increase the beam diameter, which reduces the optical power density inside the dye and at the rear mirror.

If the pulse from a mode-locked laser is too short, and one desires to stretch it, a tilted etalon can be inserted into the resonator. This will reduce the number of longitudinal modes and according to (9.4) leads to a longer pulse duration.

Liquid Dye Saturable Absorber. A saturable absorber employed for mode locking must have an absorption line at the laser wavelength, a linewidth equal to or greater than the laser line width, and a recovery time on the order of the width of the mode-locked pulses. Table 9.1 lists the recovery time and saturation flux of four dyes commonly employed in mode-locked lasers [9, 11]. For a discussion of the structure and properties of organic dyes, the reader is referred to [9, 12].

Nd:glass and Nd:YAG lasers are mode-locked with Eastman 9740, 9860 or 14015 dye suitably diluted with 1,2-dichloroethane or chlorobenzene. The dye concentration is usually chosen to produce a linear transmission between 50 and 80% at $1.06 \mu\text{m}$ through the cell. Experimental data concerning the properties of these dyes are published in [9, 13, 14].

Practically all dyes useful in the generation of mode-locked pulses decompose when exposed to ultraviolet light. In particular, Eastman 9740 and 9860 are extremely sensitive to light in the uv region. To eliminate dye breakdown due to uv radiation from flashlamp and ambient light, the dye cell should be well light-shielded with only a small aperture exposed for the laser beam. UV-absorbing

Table 9.1. Saturation density I_s and recovery time τ_s of various dyes employed for mode-locking

Dye	Eastman No. 9740	Eastman No. 9860	DDI	Cryptocyanine
I_s [W cm^{-2}]	4×10^7	5.6×10^7	$\approx 2 \times 10^7$	5×10^6
τ_s [ps]	8.3	9.3	14	22
Laser	Nd	Nd	Ruby	Ruby

glass and quartz can be used for the dye cell windows, and special uv-free fluorescent lighting around the laser area is usually installed. A suitable fluorescent lamp is the General Electric Series F96T12/Gold. Otherwise, while handling these dyes, fluorescent lights should be turned off and a tungsten-filament lamp should be used for illumination.

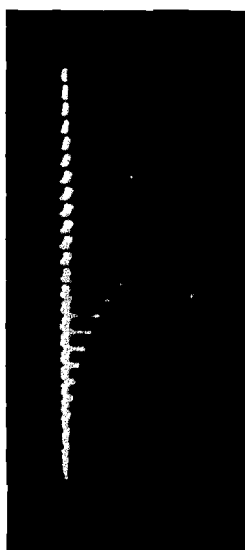
Ruby lasers are usually mode locked with either cryptocyanine or 1,1'-diethyl-2,2'-dicarbocyanine iodide (DDI). The former dye can be diluted with nitrobenzene, acetone, ethanol, or methanol. The most consistent mode-locked operation is achieved with acetone, mainly because the absorption peak for cryptocyanine in acetone exactly coincides with the ruby line, while in the other solvents it is displaced by more than 100 \AA compared to the ruby wavelength. Shorter mode-locked pulses and a more reliable operation is achieved with DDI diluted in methanol or ethanol.

Saturable absorbers should be replenished with fresh solution periodically. By far the most reliable performance from mode-locked dye systems is obtained if the dye is circulated through the cell from a large reservoir. The pumping action assures uniform mixing of the dye; because of the large volume, the dye's concentration remains constant over a long period of time and fresh dye is exposed to each laser pulse.

It has also been found that for maximum reliability of operation, it is necessary to temperature-control the dye solution. A change in absorption of 1% per degree was found in the diluted Eastman dyes 9740 and 9860. Stable and reproducible performance was achieved with a flowing dye solution temperature-controlled to $\pm 0.1^\circ\text{C}$. Such a system usually consists of a pump and temperature-controlled dye reservoir, micropore filter, and a laminar-flow dye cell. Materials which come into contact with the dye solution must be limited to stainless steel, teflon, and glass.

Gain Medium. In the past, flashlamp-pumped Nd:glass lasers have been of particular interest for mode-locking since these lasers have a broader gain bandwidth as compared to Nd:YAG and ruby, and were therefore expected to produce shorter pulses.

Typical flashlamp-pumped mode-locked Nd:glass lasers produce pulse trains about 50 to 200 ns wide, containing pulses of 5 to 20 ps in duration. The Brewster-ended rods have dimensions ranging from 8 to 20 cm in length and up to 1.5 cm in diameter. Mode locking is achieved with dye cells having a path length of

**Fig. 9.6.** Oscilloscope trace of a typical passively mode-locked Nd:glass laser. Horizontal 20 ns/div. Rise and fall times and pulse width are all detector-limited in this photograph

several millimeters. Mirrors or windows are wedged at least 30 arc/min so that they do not act as mode selectors. The total energy output can vary from 25 mJ to several hundred millijoules, and the energy content of the pulses in the middle of the train is between 1 to 10 mJ.

Figure 9.6 shows an oscilloscope trace of a typical transient passively mode-locked Nd:glass laser.

From ruby lasers of approximately similar geometry as the glass lasers mentioned above, pulse durations from 5 ps to 30 ps have been achieved. Thicknesses of dye cells range typically from several millimeters to a fraction of a millimeter. Optimum absorber cell transmission for most systems is between 0.6 and 0.8. For a typical ruby rod, 10 cm long and 1 cm in diameter, the total energy in the mode-locked pulse train is around 50 mJ and the energy per single pulse is about 2 to 5 mJ in the center of the train.

Mode-locked Nd:YAG lasers typically employ laser rods ranging from $3 \times 5 \text{ mm}$ to $6 \times 75 \text{ mm}$ in size. With 1-mm-thick dye cells pulses between 20 and 40 ps in duration have been produced. Depending on dye concentration and flashlamp energy, the pulse trains are usually 10 to 80 ns long. Figure 9.7a shows a typical mode-locked train generated by a Nd:YAG laser. A portion of the pulse in the center was switched out in order to measure the pulse width. Figures 9.7b and c show an oscillogram and a two-photon absorption measurement of this pulse.

Despite the relatively simple construction of a passively mode-locked laser oscillator, the output will be very unpredictable unless dye concentration, optical pumping intensity, and resonator alignment are carefully adjusted. It is not uncommon to find that the average pulse duration from one train of picosecond pulses to the next changes significantly and that the pulse train envelopes are not reproducible. For instance, one may find that, in ≈ 10 shots, optimum mode locking occurred only once. With the proper saturable absorber and with a judiciously chosen optical system, the probability of obtaining clean mode-locked pulse trains which are free of subsidiary pulses is typically 0.6 to 0.7 in pulsed passively mode-locked solid-state lasers. Furthermore, mixing and handling the dye solution and maintaining proper dye concentration proved cumbersome. As